A New Perspective of the Physical Processes Associated with the Clear-Sky Greenhouse Effect over High Latitudes

Zuohao CAO*[1], Ronald E. STEWART[2], and M. K. YAU[2]

[1] *Meteorological Service of Canada, Ontario, Canada*

[2] *Department of Atmospheric and Oceanic Sciences, McGill University Montreal, Quebec, Canada*

(Received 21 June 2003; revised 26 August 2003)

ABSTRACT

The physical processes associated with the clear-sky greenhouse effect in the presence of water vapor are examined by including surface emissivity in the greenhouse effect formulation, and by introducing a new way to partition physical processes of the greenhouse effect. In this new framework, it is found that the clear-sky greenhouse effect is governed by three physical processes associated with (1) the temperature contrast between the surface and the atmosphere, (2) the interaction between the surface emissivity and the temperature contrast, and (3) the surface emissivity. The importance of the three physical processes is assessed by computing their vertical and spectral variations for the subarctic winter and summer standard atmosphere using the radiation model MODTRAN3 (Moderate Resolution Transmittance code Version 3). The results show that the process associated with the temperature contrast between the surface and the atmosphere dominates over the other two processes in magnitude. The magnitude of this process has substantial variations in the spectral region of 1250 to 1880 cm^{-1} and in the far infrared region. Due to the low-level temperature inversion over the subarctic winter, there exists a negative contribution to the greenhouse trapping. The seasonal variations are, however, dominated by the processes associated with the interaction between the surface emissivity and the temperature contrast as well as the surface emissivity itself. The magnitudes of these two physical processes contributing to the greenhouse trapping over the subarctic winter are about 7 to 10 times of those over the subarctic summer, whereas the magnitude of the processes associated with the temperature contrast in the subarctic summer is only about 2 times of that in the subarctic winter.

Key words: greenhouse effect, surface emissivity, physical processe, high latitude, seasonal variation

1. Introduction

The greenhouse effect is defined as the difference in upwelling longwave radiation between the surface and the top of the atmosphere (TOA). If E represents the longwave emission from the surface, and F represents the emission from TOA, then the absolute forcing of the climate system due to greenhouse effect, G, is given by $G=E-F$. Based on Hallberg and Inamdar (1993), the greenhouse effect can be derived from the radiative transfer equations which apply to blackbody longwave emission

$$G=2\pi\int_0^{\infty}\int_0^{1}\int_0^{\tau_\lambda^*}[B_\lambda(T_\mathrm{s})-B_\lambda(T)]e^{-\frac{\tau}{\mu}}d\tau d\mu d\lambda\,, \quad (1)$$

where $B_\lambda(T_\mathrm{s})$ and $B_\lambda(T)$ are the Planck functions at surface temperature T_s and atmospheric temperature T, $\mu(=\cos\theta)$ is the cosine of the angle from the vertical, and τ_λ^* is the total optical depth of the atmosphere at wavelength λ. Note that TOA (Hallberg and Inamdar, 1993; Raval and Ramanathan, 1989; and many others) instead of the tropopause (IPCC, 1990) is used in Eq. (1) so that it can include the effects of other important upper-level greenhouse gases such as ozone. The magnitude of the greenhouse effect may be estimated by taking the difference between E and F. The global/annual average values of E and F are, respectively, 390 W m^{-2} (Stephens and Tsay, 1990) and 235 W m^{-2} (Harrison et al., 1990), giving a G value about 155 W m^{-2}. The clear-sky value of F in the global/annual average is 265 W m^{-2} (Harrison et al., 1990). Thus, the clear-sky greenhouse effect is 125 W m^{-2}. The contribution of clouds to the greenhouse effect is about 30 W m^{-2} (Harrison et al., 1990). This

*E-mail: zuohao.cao@ec.gc.ca

indicates that the magnitude of the longwave trapping is largely controlled by the gaseous constituents of the atmosphere, in particular water vapor, under a clear-sky condition. It is clear from Eq. (1) that the clear-sky greenhouse effect is sensitive to changes in surface temperature, atmospheric temperature, and greenhouse gases.

The transmittance ($e^{-\frac{\tau}{\mu}}$), associated with the integrated concentration of greenhouse gases such as water vapor, is usually targeted by scientists for examining greenhouse warming. Although water vapor in the atmosphere is a very small fraction of the total air mass, it plays very important roles in midlatitude precipitating systems (e.g., Cao and Cho, 1995), and it acts as a powerful greenhouse gas (e.g., Harries, 1997; Chahine, 1992) and nearly doubles the effects of greenhouse warming caused by carbon dioxide, methane, and all similar gases (Manabe and Wetherald, 1967; Raval and Ramanathan, 1989). The effect of water-vapor-feedback on greenhouse warming is, however, still under debate (Raval and Ramanathan, 1989; Stephens, 1990; Lindzen, 1990; Rind et al., 1991; Stephens and Greenwald, 1991; Hallberg and Inamdar, 1993; Inamdar and Ramanathan, 1994; Stephens et al., 1993; Mitchell et al., 1995; Slingo and Webb, 1997). One particular focus of the debate is on whether over tropical oceans moisture evaporated from the warm sea surface can be transported into the free atmosphere by convection, and whether downdraughts associated with the convection dry the upper troposphere.

The geographical distribution of the greenhouse effect is governed by the concentration of water vapor and its distribution in association with dynamics; it is also governed by the thermodynamics associated with longwave radiation at the surface as well as in the atmosphere ($B_\lambda(T_\mathrm{s})-B_\lambda(T)$). To reduce the complexity in dealing with the surface and the atmosphere longwave radiation, most researchers (e.g., Hallberg and Inamdar, 1993, and many others) have treated them as blackbody emission as a first approximation although the clear-sky emissivity can be expressed as a complicated function of water vapor pressure, dew point temperature, and so on (Berger et al., 1984; Martin and Berdahl, 1984). This treatment is reflected in the definition of the greenhouse effect in Eq. (1).

Although the blackbody approximation captures most features of the land surface's longwave radiation, some critical characteristics are still missing. As an important input of longwave radiation into the atmosphere, longwave emission from the land surface is critically dependent on the surface emissivity and its variations with season. Especially over high latitudes where substantial seasonal cycles occur in the alteration of vegetation and snow cover, the atmospheric longwave trapping will have corresponding seasonal variations. Furthermore, vegetation and snow significantly influence the changes of atmospheric moisture contents, respectively, through evaporation during the growing season, sublimation in the winter, and allocations to other hydrological components (e.g., Cao et al., 2002).

Since the land surface is a greybody, it is able to reflect the downward atmospheric radiation with a reflection ratio of $1-\varepsilon_s$ (ε_s is the surface emissivity). To be consistent with the greybody emission, this effect should be considered as a process contributing to the greenhouse effect although the reflection of the downward atmospheric radiation is quite often omitted in the infrared region (Fouquart and Vesperini, 1996) because the surface reflection is often very small in the infrared region and the downward atmospheric radiation is much smaller than the surface emission itself in a clear-sky condition (Fouquart and Vesperini, 1996).

After considering the above surface forcing, the definition of the greenhouse effect in Eq. (1) should be modified to become

$$G = 2\pi \int_0^\infty \int_0^1 \int_0^{\tau_\lambda^*} \{[\varepsilon_\mathrm{s} B_\lambda(T_\mathrm{s}) - B_\lambda(T)] e^{-\frac{\tau}{\mu}} + (1-\varepsilon_\mathrm{s}) B_\lambda(T) e^{-\frac{(\tau_\lambda^*-\tau)}{\mu}}\} d\tau d\mu d\lambda \,, \qquad (2)$$

It is clear that the greenhouse effect is also sensitive to surface emissivity. The focus of this paper is to consider a more realistic surface radiative forcing in the framework of Eq. (2), and to ask the question of what is new compared with the traditional definition of Eq. (1).

In this new configuration where the greenhouse effect is defined as Eq. (2), our objectives are to examine the physical processes associated with the greenhouse effect over high latitudes. These include land surface processes through non-blackbody emissivity, the temperature contrast between the surface and the atmosphere, and possible interactions between them. Although the surface emissivity plays an important role in contributing to the greenhouse effect, the influence is still poorly understood, particularly over high latitudes where the surface coverage has significant seasonal variations. In this study, the effect of the surface emissivity on the greenhouse effect will be examined.

Since the greenhouse effect is dependent on the difference of longwave radiation at the surface and in the atmosphere, the temperature contrast between the surface and the atmosphere is an important measure of the strength and the seasonal variation of the greenhouse effect. Particularly over the high latitudes during the winter periods, the effect of water vapor on the net flux of radiation is complicated by the presence of

a temperature inversion (Curry et al., 1995). It was qualitatively pointed out by Curry et al. (1995) that the greenhouse effect will be smaller for a stronger inversion due to the cold surface temperature relative to the atmospheric temperature. However, little work has been done on the explicit formulation of the effect of this temperature contrast on the greenhouse effect and corresponding computations using radiative transfer models. In this study, we will shed further light on this issue. Particularly in the presence of vegetation and snow over a seasonal cycle, the effect of this temperature contrast may be enhanced or reduced.

As pointed out by Shindell et al. (1998), increasing greenhouse gases in the troposphere may lead to severe ozone depletion over both poles due to greenhouse-gas-induced lower-stratospheric cooling. This suggests that the position and strength of the greenhouse gas warming and its temporal variation over high latitudes may be somewhat related to ozone holes. Hence, it is important to understand the physical processes controlling the greenhouse effect over high latitudes.

Our approach is to derive a new formulation for the greenhouse effect to better understand the underlying physical processes and possible interactions among them. Computational examples are shown by employing a radiation model (MODTRAN) with the input data from a model atmosphere.

2. Physical processes of the greenhouse effect

We derive a new expression for the greenhouse effect by substituting the Planck function

$$B_\lambda(T) = \frac{C_1}{\lambda^5}\frac{1}{e^{\frac{C_2}{\lambda T}} - 1} ,$$

where

$$C_1 = 2hC^2 (= 1.191 \times 10^8 \text{ W m}^{-2} \text{ sr}^{-1} \ \mu\text{m}^4) ,$$

$$C_2 = \frac{hC}{k} (= 1.439 \times 10^4 \text{ K } \mu\text{m}) ,$$

and C, h, and k are, respectively, the speed of light, and the Planck and Boltzmann constants into Eq. (2), and rearranging the resulting equation and making use of mathematical identities; we yield

$$G = \int_0^\infty \int_0^1 \int_0^{\tau_\lambda^*} G_\text{p} d\tau d\mu d\lambda , \qquad (3)$$

where

$$\begin{aligned} G_\text{p} = 2\pi \{ & \underbrace{B_\lambda(T)[1+\frac{\lambda^5}{C_1}B_\lambda(T_\text{s})](e^{\frac{C_2}{\lambda}(\frac{T_\text{s}-T}{TT_\text{s}})} - 1)}_{\text{term 1}} \\ & \underbrace{- B_\lambda(T)[1+\frac{\lambda^5}{C_1}B_\lambda(T_\text{s})](1-\varepsilon_\text{s})(e^{\frac{C_2}{\lambda}(\frac{T_\text{s}-T}{TT_\text{s}})} - 1)}_{\text{term 2}} \\ & \underbrace{- B_\lambda(T)(1-\varepsilon_\text{s})(1-e^{-\frac{\tau_\lambda^*-2\tau}{\mu}})}_{\text{term 3}} \} e^{-\frac{\tau}{\mu}} . \end{aligned} \qquad (4)$$

The terms in Eq. (2) are now formulated in three terms in Eq. (4), which allows us to partition the physical processes associated with the greenhouse effect. These three processes are, respectively, governed by: (1) the temperature contrast, between the surface and the atmosphere, (2) the interaction between the surface emissivity and the temperature contrast, and (3) the surface emissivity.

2.1 *The temperature contrast*

Under the assumptions that the surface and the atmospheric longwave radiation can be treated as blackbody emission, the first term in Eq. (4) is an exact formulation of the greenhouse effect defined by Eq. (1). When the surface temperature is greater than the atmospheric temperature, there is a positive contribution to the greenhouse effect. Otherwise, a negative contribution results.

It is important to keep all the important physical processes to avoid the problems of making unrealistic assumptions in the study of the greenhouse effect. For example, under the assumption of constant atmospheric temperature T for the entire atmosphere (e.g., Webb et al., 1993), there will be no vertical variation of atmospheric temperature. The longwave trapping is therefore always positive under this assumption since the average atmospheric temperature T over a deep column is always less than the surface temperature. However, during the winter over high latitudes, the common occurrence of a strong low-level temperature inversion can change the sign as well as the magnitude of the longwave trapping. An atmosphere with a constant temperature cannot be used to model such behavior.

Note that in the first term of Eq. (4), the sole factor which determines the sign of the greenhouse trapping is the temperature difference between the surface and the atmosphere, and not the lapse rate as stated in Raval and Ramanathan (1989). In deriving their Eq. (1), they assumed that the surface temperature is identical to the air temperature at the surface (see Rodgers, 1967). This assumption leads to the finding

that the lapse rate is the sole factor determining the sign of the greenhouse effect.

2.2 *The surface emissivity*

The second and the third terms in Eq. (4) usually make a negative contribution to the greenhouse effect because $1-\varepsilon_s$ is mainly positive.

The net effect of the surface emissivity on the greenhouse effect can be obtained by combining the three terms in Eq. (4). By doing this, we yield

$$G = 2\pi \int_0^{\infty} \int_0^{1} \int_0^{\tau_\lambda^*} \{\varepsilon_s B_\lambda(T)[1+\frac{\lambda^5}{C_1} B_\lambda(T_s)](e^{\frac{C_2}{\lambda}(\frac{T_s-T}{TT_s})} - 1) - B_\lambda(T)(1-\varepsilon_s)(1-e^{-\frac{\tau_\lambda^*-2\tau}{\mu}})\} e^{-\frac{\tau}{\mu}} d\tau d\mu d\lambda \,. \quad (5)$$

When blackbody emission (ε_s=1) is assumed, however, the first term in the above equation only describes the effect of the temperature contrast on the greenhouse trapping. It can be shown that Eq. (5) is identical to Eq. (1) when ε_s is equal to 1. In other words, the definition of the greenhouse effect using Eq. (1) cannot capture the interaction between the surface emissivity and the temperature contrast.

3. The radiation model, input data, and numerical experiments

The MODTRAN3 radiative transfer model (Anderson et al., 1994) was used to calculate atmospheric transmittance and longwave radiation. The accuracy of the MODTRAN model was tested by meticulously comparing its results with FASCODE (Fast Atmospheric Signature Code) (a line-by-line radiation model) calculations (Kneizys et al., 1996). For most observational conditions and spectral domains, the accuracy of the MODTRAN transmittance calculations falls within a few percent of the predictions by FASCODE, in both statistical and spectral details (Kneizys et al., 1996). The MODTRAN calculations were also compared with actual measurements. The agreement, except for the 10-μm ozone band, is within a few percent in the root-mean-square sense (Kneizys et al., 1996).

The dataset used in this study for the radiative transfer computations was obtained from the model atmosphere data used for the intercomparison of radiation codes in climate models (Ellingson et al., 1991). This dataset provides temperature and moisture information up to a height of 103 km. As shown in Fig. 1a, during the winter the temperature over the subarctic generally decreases with height in the troposphere except at the lower levels where the temperature inversion occurs. It has been documented that the temperature inversion over high latitudes during the winter can be extended up to about the 700-hPa pressure surface (Cao et al., 2001). Over the summer, however, the temperature inversion does not appear at the low levels of the subarctic atmosphere (Fig. 1c). As expected, there is a strong seasonal variation of moisture content over the subarctic atmosphere. Comparisons between Fig. 1b and Fig. 1d indicate that the moisture content in the summer is almost 10 times larger than that in the winter.

Simulations have been performed over the range from wavenumber 0 to 2500 cm^{-1} at a resolution of 10 cm^{-1}. Recently, it has been found that the far infrared component (defined as wavelengths greater than about 20 μm) of the water vapor spectrum may have a significant influence on the water vapor greenhouse effect (Clough et al., 1992; Sinha and Allen, 1994), particularly for the subarctic winter (SAW) atmosphere (Sinha and Harries, 1995). Maximum water vapor greenhouse trapping arises in the far infrared over the middle/upper troposphere (Sinha and Harries, 1995).

The magnitude of the surface emissivity is highly dependent on seasonal variations in surface coverage. However, observations of surface emissivity with various surface coverages over all wavelengths are not fully available, in particular there is a lack of observations over the far infrared regions. Since the focus of this study is not on the emissivity itself, the values of the surface emissivity are directly obtained from the available publications. In this paper, we only take into account the currently available observations of surface emissivity data, not model outputs. For example, green vegetation has a high emissivity value and a low spectral variability (Rubio et al., 1997). The average value of the vegetation emissivity of 0.985 over the region of 3 to 13 μm (Caselles et al., 1997) was used in this study. However, snow emissivity varied considerably during the winter (Rees, 1993). Rees (1993) observed the winter snow emissivity being 0.70 whereas Kondo and Yamazawa (1986) measured the winter snow emissivity as 0.98. In this study, an average value (0.84) of Rees (1993) and Kondo and Yamazawa (1986) was used for the winter snow emissivity since it may represent a mean status of the winter snow emissivity. Because our focuses in this study are on the greenhouse effect and its associated physical processes under mean atmospheric and surface conditions, the average atmospheric temperature and moisture profiles and the average surface emissivity are used. The sensitivity of the greenhouse effect to the surface emissivity is further examined in section 4.

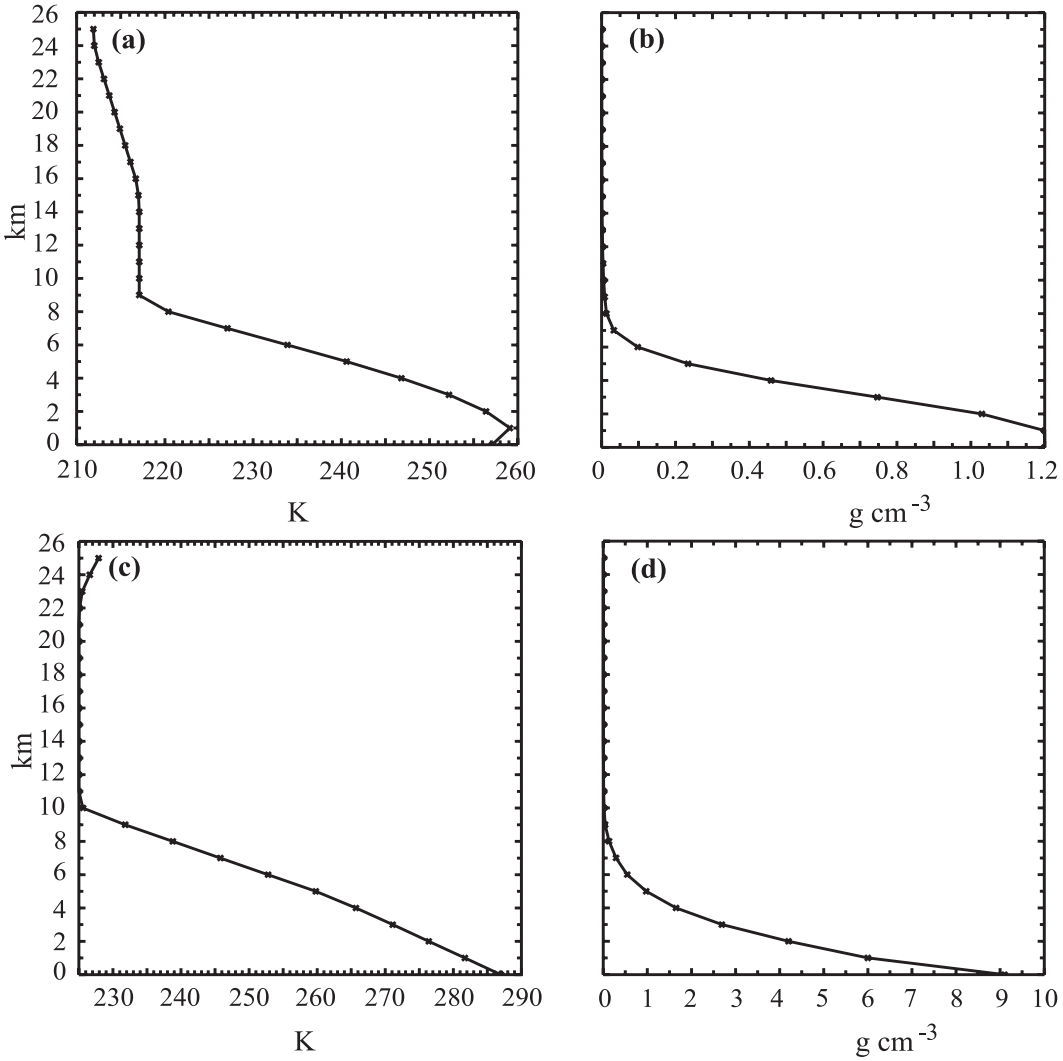

Fig. 1. Vertical profiles for the subarctic winter of (a) temperature (K) and (b) moisture (g cm^{-3}) and vertical profiles for the subarctic summer of (c) temperature (K) and (d) moisture (g cm^{-3}).

4. Results

In section 4.1, the spectral, vertical, and seasonal variations of the three terms in Eq. (4) are presented, and in section 4.2, the spectral and vertical integrations of these three terms are performed to understand their contributions to the greenhouse effect. In both sections, computations are carried out over the whole model atmosphere column, although features in Figs. 2 and 3 are shown up to 24 km due to little change above this height.

4.1 *Spectral, vertical, and seasonal variations*

All the individual terms in Eq. (4) are computed to evaluate the relative importance of those physical processes associated with the greenhouse effect. Figure 2 shows spectral and vertical variations of these terms in Eq. (4) for the subarctic winter atmosphere. At the lower levels of the troposphere where the temperature inversion occurs, there is a non-negligible negative contribution to the greenhouse trapping, particularly over the spectrum approximately from 350 to 1420 cm^{-1}. This negative contribution to the greenhouse effect is due to the low-level temperature inversion occurring over high latitudes during the winter. The negative contribution extends up to the height at which the atmospheric temperature is equal to the surface temperature (about 1.5 km as shown in Fig. 2a). Since it is common for a low-level temperature inversion to occur in the winter over high latitudes (Cao et al., 2001), the negative contribution to the greenhouse effect due

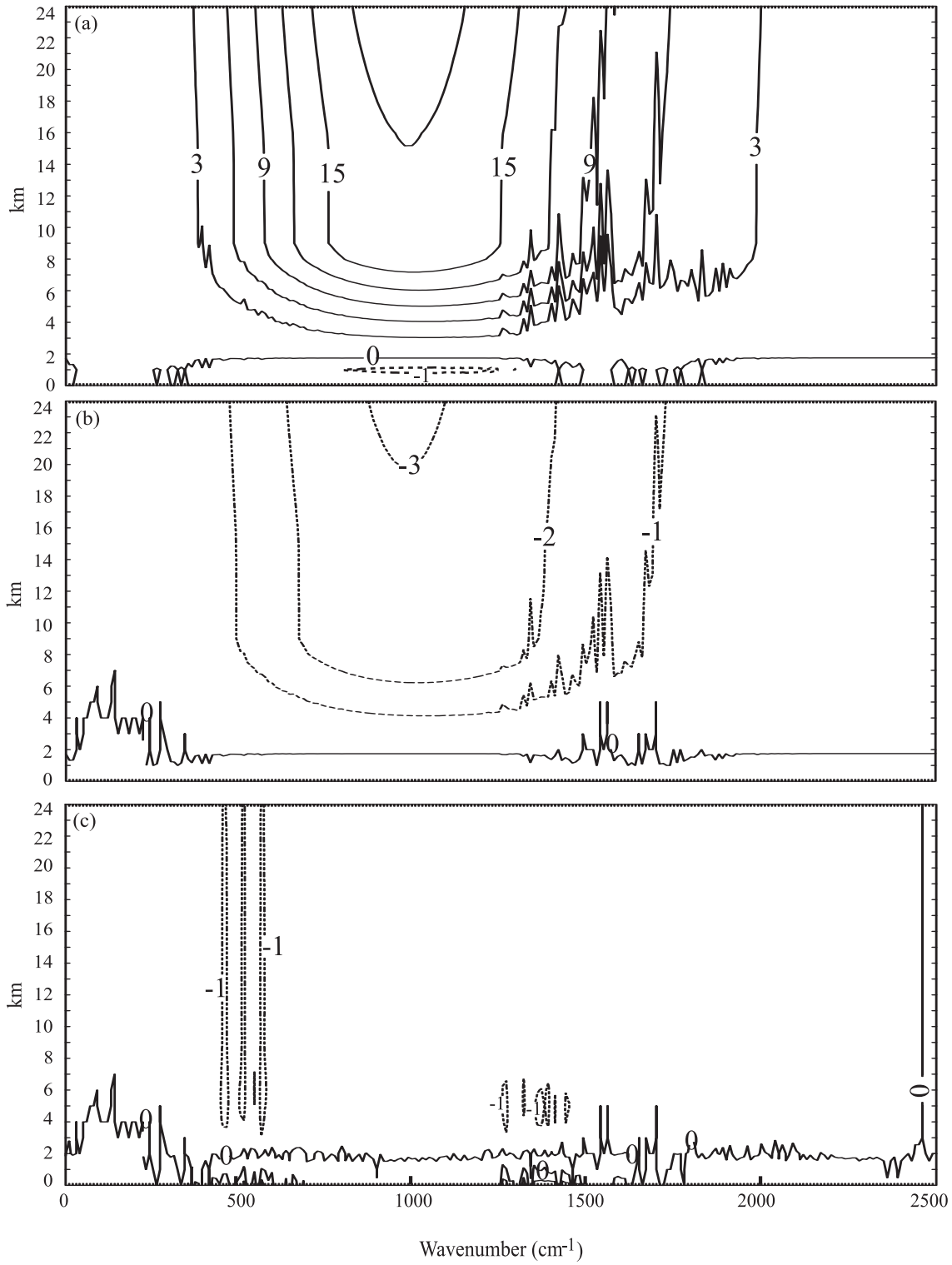

Fig. 2. Vertical-spectral variations for the subarctic winter of the terms in Eq. (4): (a) term 1 associated with the temperature contrast at intervals of 3 W m^{-2} μm^{-1} for positive values and –1 W m^{-2} μm^{-1} for negative values, (b) term 2 associated with the interaction between the surface emissivity and the temperature contrast at intervals of –1 W m^{-2} μm^{-1}, and (c) term 3 associated with the surface emissivity at intervals of –1 W m^{-2} μm^{-1}.

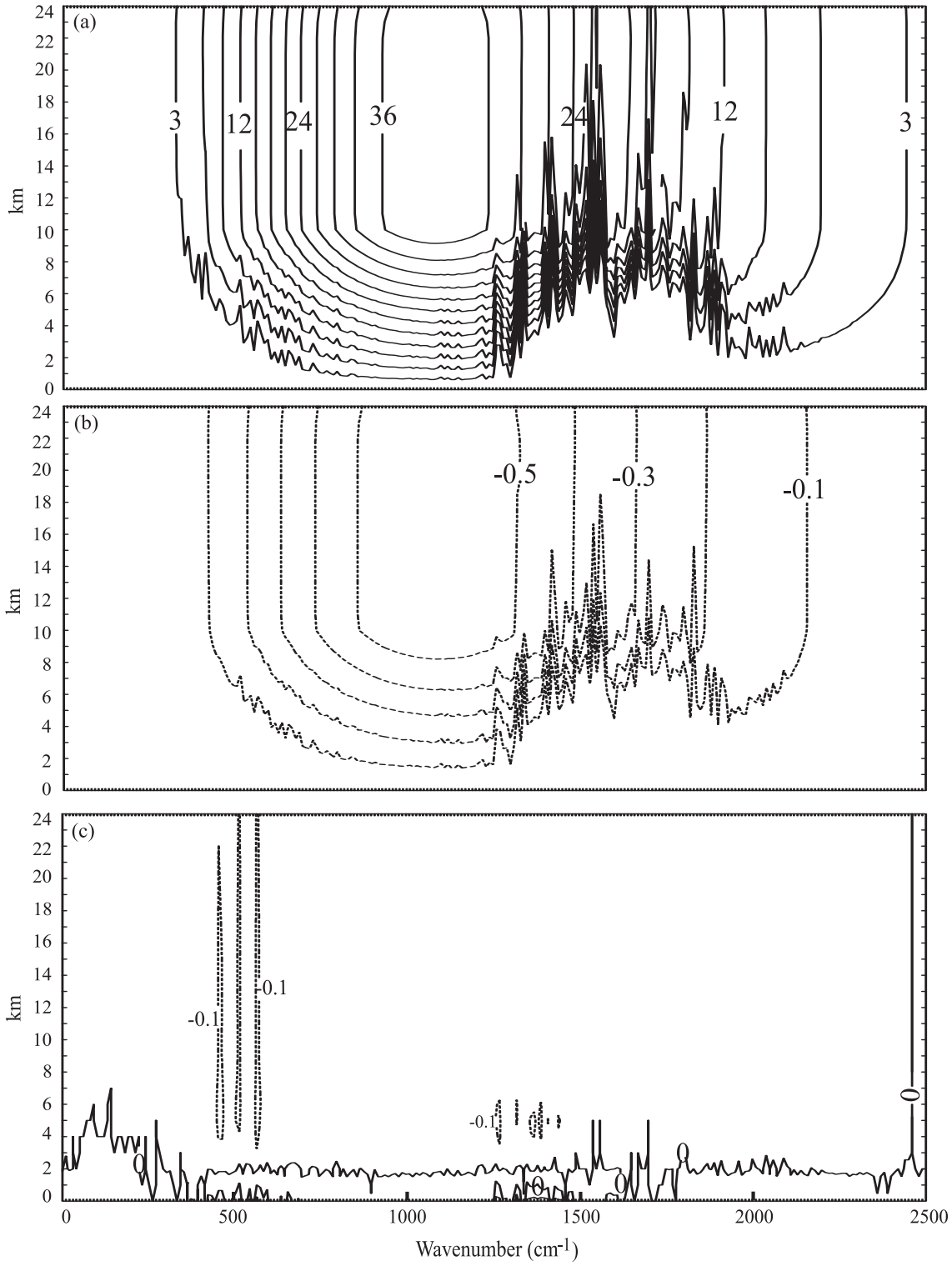

Fig. 3. Vertical-spectral variations for the subarctic summer of terms in Eq. (4): (a) term 1 associated with the temperature contrast with a contour interval of 3 W m^{-2} μm^{-1}, (b) term 2 associated with the interaction between the surface emissivity and the temperature contrast with a contour interval of –0.1 W m^{-2} μm^{-1}, and (c) term 3 associated with the surface emissivity with a contour interval of –0.1 W m^{-2} μm^{-1}.

to this temperature structure is important. At the upper levels of the troposphere, however, the first term of Eq. (4) generally increases with height especially over the spectrum of 500 to 1250 cm^{-1}. Beyond this region, there are two spectral regions, 300 to 500 cm^{-1} and 1250 to 1880 cm^{-1}, demonstrating fluctuations. The perturbation of the former is smaller in magnitude than that of the latter mainly due to the low intensity of the Planck function at the former spectral region although vertical variation of transmittance is strong at this region. The perturbation in the latter region reflects the vertical variations of transmittance and moisture contents. Above the troposphere, the increase of the first term is mainly confined to the spectral region of about 850 to 1100 cm^{-1}, with substantial fluctuations in the region of 1330 to 1880 cm^{-1}.

Comparisons between two seasons (Fig. 2a and Fig. 3a) indicate that the process associated with the temperature contrast in the summer is about 2 times larger than that in the winter although they are of the same order of magnitude. No negative contributions are observed in the summer because the low-level temperature inversion does not occur in the subarctic summer atmosphere. Similar to the winter, the fluctuations appear in two spectral regions over the summer, which are almost located in the same regions as those in the winter. The perturbations in these two regions over the summer are much stronger than those over the winter since the temperature contrast between the surface and atmosphere is stronger in the summer. It is also observed that these two spectral regions are broader in the summer than those in the winter.

The second term, associated with the surface emissivity and the temperature contrast, has negative contributions with the same order of magnitude as the first term over the winter (Fig. 2b and Fig. 2a). This indicates that the interaction between the surface emissivity and the temperature contrast is important during the winter. The magnitude of the absolute values of this term increases with height in the troposphere over the spectral region of about 500 to 1750 cm^{-1} (Fig. 2b). The fluctuations occur in the spectral region of approximately 1250 to 1750 cm^{-1}. These fluctuations can extend up to about 15 km.

It is very interesting to note that the process associated with the surface emissivity and the temperature contrast has very significant seasonal variations. This term in the winter is about 6 times larger than that in the summer (see Fig. 2b and Fig. 3b). These seasonal variations are mainly due to surface emissivity changes over the two seasons (snow versus vegetation) and their interactions with the temperature contrasts.

The third term, associated with the surface emissivity, demonstrates that the fluctuations are confined to two spectral regions, approximately 500 cm^{-1} and 1250–1500 cm^{-1} (Fig. 2c and Fig. 3c). Also, this term displays significant seasonal variations, and its magnitude over the winter is about 10 times larger than that over the summer.

In short, the seasonal variations of the second and third terms are much stronger than those of the first term although the magnitude of the first term is larger. This statement is also valid even for a large value of ε_s=0.9.

The relative importance of physical processes in Eq. (4) is evaluated over the wavenumber from 0 to 2500 cm^{-1}. Since the observational surface emissivity is only available over infrared regions in the literature, the surface emissivity of snow and vegetation in the infrared region is used in this paper. It is clear that observations of the surface emissivity over the far infrared regions are needed to eliminate the uncertainty in evaluation of the importance of the various physical processes in Eq. (4).

4.2 *Spectral and vertical integration*

The spectrally and vertically integrated values of the three parts of the greenhouse effect and the total greenhouse effect (G) are computed for the subarctic winter and summer (Table 1). Comparisons between the two subarctic seasons indicate that the magnitudes of the second and third terms contributing to the greenhouse trapping over the subarctic winter are about 7 to 10 times those over the subarctic summer, whereas the magnitude of the first term in the subarctic summer is only about 2 times that in the subarctic winter.

5. Conclusions

Different from the earlier studies (Raval and Ramanathan, 1989; Sinha and Harries, 1995) where the surface longwave radiation is treated as the blackbody emission, it is considered to be a greybody emission in this paper. In contrast to the previous research that paid attention to water vapor greenhouse trapping over different spectral regions (e.g., an infrared region of Raval and Ramanathan (1989) and a far

Table 1. Variations of the spectrally and vertically integrated values of the three parts of the greenhouse effect and the total (in units of W m^{-2}) over the subarctic winter and summer.

	Winter	Summer
Term 1	89.7	147.5
Term 2	–14.4	–2.2
Term 3	–11.3	–1.1
Total	64.1	144.3

infrared region of Sinha and Harries (1995)), the focus of this paper is on the physical processes and their seasonality in contributing to the greenhouse trapping and its seasonal variations, particularly when the surface emissivity is taken into account. By introducing the surface emissivity into the formulation, we have defined a new expression for the greenhouse effect. Based on the new formulation, the greenhouse trapping has been partitioned into three physical processes. These are associated with (1) the temperature contrast between the surface and the atmosphere, (2) the interaction between the surface emissivity and the temperature contrast, and (3) the surface emissivity.

Numerical simulations with the aid of the radiation model MODTRAN3 show that the process associated with the temperature contrast between the surface and the atmosphere dominates over the other two processes. Over the subarctic winter, the low-level temperature contrast is substantially reduced due to the temperature inversion and this results in a negative contribution to the greenhouse effect. The magnitude of this process is highly perturbed in the spectral region of 1250 to 1880 cm^{-1} as well as in the far infrared region. The dominant seasonal variations are, however, associated with processes of the interaction between the surface emissivity and the temperature contrast as well as the surface emissivity itself. The magnitudes contributing to the greenhouse effect due to this interaction and the surface emissivity itself over the winter are about 7 to 10 times those over the subarctic summer.

This research has demonstrated the importance of the surface emissivity and its seasonality in contributing to the greenhouse trapping and its seasonal variations. It is suggested that the availability of more surface emissivity data over various spectral regions (e.g., the far infrared region) is a key to yield further insight into the roles played by the surface emissivity in contributing to the greenhouse effect and associated climate variability and change. In the future, this research will be applied to investigations of the longterm effects of the surface emissivity on greenhouse trapping using observed data.

Acknowledgments. This research was supported in part by the Panel on Energy Research and Development (PERD) and by Environment Canada through the Mackenzie GEWEX Study (MAGS). The authors would like to thank Marc Fournier for his help with the computations using MODTRAN3. Thanks are also extended to the anonymous reviewers for their comments and suggestions that have improved this paper.

REFERENCES

Anderson, G. P., and coauthors, 1994: MODTRAN3: Suitability as flux-divergence code. *Proc. of the 4th ARM Science Team Meeting*, Charleston, S. C.

Berger, X., D. Buriot, and F. Garnier, 1984: About the equivalent radiative temperature for clear skies. *Solar Energy*, **29**, 299–314.

Cao, Z., and H.-R. Cho, 1995: Generation of moist potential vorticity in extratropical cyclones. *J. Atmos. Sci.*, **52**, 3263–3281.

Cao, Z., R. E. Stewart, and W. D. Hogg, 2001: Extreme winter warming events over the Mackenzie basin: Dynamic and thermodynamic contributions. *J. Meteor. Soc. Japan*, **79**, 785–804.

Cao, Z., M. Wang, B. A. Proctor, G. S. Strong, R. E. Stewart, H. Ritchie, and J. E. Burford, 2002: On the physical processes associated with the water budget and discharge of the Mackenzie Basin during the 1994/1995 water year. *Atmos.-Ocean*, **40**, 125–143.

Caselles, V., E. Valor, C. Coll, and E. Rubio, 1997: Thermal band selection for the PRISM instrument 1. Analysis of emissivity-temperature separation algorithms. *J. Geophys. Res.*, **102**, 11145–11164.

Chahine, M. T., 1992: The hydrological cycle and its influence on climate. *Nature*, **359**, 373–380.

Clough, S. A., M. J. Iacono, and J.-L. Moncet, 1992: Line-by-line calculations of atmospheric fluxes and cooling rates: Application to water vapor. *J. Geophys. Res.*, **97**, 15761–15785.

Curry, J. A., J. L. Schramm, M. C. Serreze, and E. E. Ebert, 1995: Water vapor feedback over the Arctic Ocean. *J. Geophys. Res.*, **100**, 14223–14229.

Ellingson, R. G., J. Ellis, and S. Fels, 1991: The intercomparison of radiation codes used in climate models: Longwave results. *J. Geophys. Res.*, **96**, 8929–8953.

Fouquart, Y., and M. Vesperini, 1996: Principles of active and passive remote measurements of water in the atmosphere and at ground. *Radiation and Water in the Climate System*. Springer, 614pp.

Hallberg, R., and A. K. Inamdar, 1993: Observations of seasonal variations in atmospheric greenhouse trapping and its enhancement at high sea surface temperature. *J. Climate*, **6**, 920–931.

Harries, J. E., 1997: Atmospheric radiation and atmospheric humidity. *Quart. J. Roy. Meteor. Soc.*, **123**, 2173–2186.

Harrison, E. F., P. Minnis, B. R. Barkstrom, V. Ramanathan, R. Cess, and G. G. Gibson, 1990: Seasonal variation of cloud radiative forcing derived from the Earth Radiation Budget Experiment. *J. Geophys. Res.*, **95**, 18687–18703.

Inamdar, A. K., and V. Ramanathan, 1994: Physics of greenhouse effect and convection in warm oceans. *J. Climate*, **7**, 715–731.

IPCC, 1990: Climate Change: The IPCC Scientific Assessment. Report Prepared for Intergovernmental Panel on Climate Change, WMO/UNEP, Cambridge University Press, 362pp.

Kneizys, F. X., and coauthors, 1996: The MODTRAN 2/3 report and LOWTRAN 7 model. Report Name and number, total number [Available from Phillips Laboratory, Geophysics Directorte, PL/GPOS, 29 Randolph Road, Hanscom AFB, MA 01731-3010.]

Kondo, J., and H. Yamazawa, 1986: Measurement of snow surface emissivity. *Bound.-Layer Meteor.*, **71**, 288-299.

Lindzen, R. S., 1990: Some coolness concerning global warming. *Bull. Amer. Meteor. Soc.*, **71**, 288–299.

Manabe, S., and R. T. Wetherald, 1967: Thermal equilibrium of the atmosphere with a given distribution of relative humidity. *J. Atmos. Sci.*, **24**, 241–259.

Martin, M., and P. Berdahl, 1984: Characteristics of infrared sky radiation in the United States. *Solar Energy*, **33**, 321–336.

Mitchell, J. F. B., T. C. Johns, J. M. Gregory, and S. Tett, 1995: Climate response to increasing levels of greenhouse gases and sulphate aerosols. *Nature*, **376**, 501–504.

Raval, A., and V. Ramanathan, 1989: Observational determination of the greenhouse effect. *Nature*, **342**, 758–762.

Rees, W. G., 1993: Infrared emissivity of Arctic winter snow. *Int. J. Remote Sens.*, **14**, 3069–3073.

Rind, D., E. W. Chiou, W. Chu, J. Larsen, S. Oltmans, J. Lerner, M. P. McCormick, and L. McMaster, 1991: Positive water vapor feedback in climate models confirmed by satellite data. *Nature*, **349**, 500–503.

Rodgers, C. D., 1967: The use of emissivity in atmospheric radiation calculations. *Quart. J. Roy. Meteor. Soc.*, **93**, 43–54.

Rubio, E., 1997: Emissivity measurements of several soils and vegetation types in the 8-14 μm wave band: Analysis of two field methods. *Remote Sens. Environ.*, **59**, 490–521.

Shindell, D. T., D. Rind, and P. Lonergan, 1998: Increased polar stratospheric ozone losses and delayed eventual recovery owing to increasing greenhouse-gas concentrations. *Nature*, **392**, 589–592.

Sinha, A., and M. R. Allen, 1994: Climate sensitivity and tropical moisture distribution. *J. Geophys. Res.*, **99**, 3707–3716.

Sinha, A., and J. E. Harries, 1995: Water vapor and greenhouse trapping: The role of far infrared absorption. *Geophys. Res. Lett.*, **22**, 2147–2150.

Slingo, A., and M. J. Webb, 1997: The spectral signature of global warming. *Quart. J. Roy. Meteor. Soc.*, **123**, 293–307.

Stephens, G. L., 1990: On the relationship between water vapor over the oceans and sea surface temperature. *J. Climate*, **3**, 634–645.

Stephens, G. L., and S.-C. Tsay, 1990: On the cloud absorption anomaly. *Quart. J. Roy. Meteor. Soc.*, **116**, 671–704.

Stephens, G. L., and T. J. Greenwald, 1991: The Earth's radiation budget and its relation to atmospheric hydrology: 1: Observations of the clear-sky greenhouse effect. *J. Geophys. Res.*, **96**, 15325–15340.

Stephens, G. L., D. A. Randall, I. L. Wittmeyer, and D. A. Dazlich, 1993: The Earth's radiation budget and its relation to atmospheric hydrology: 3: Comparison of observations over the oceans with a GCM. *J. Geophys. Res.*, **98**, 4931–4950.

Webb, M. J., A. Slingo, and G. L. Stephens, 1993: Seasonal variations of the clear-sky greenhouse effect: The role of changes in atmospheric temperature and humidities. *Climate Dyn.*, **9**, 117–129.